

Research Paper

Integrating Remote Sensing and Field Observations for Karst Morphological Analysis: Evidence from Rongkop, Gunung Kidul

Utama, P. P.¹, Adha, I.¹, Dewi, N. K. E. S.², Anggrasari, H.³, Ajie, M. A.¹, Zelvany, Z. T.¹, Adelina, J. G.1, Ginting, L. M.1

- ¹ Department of Geological Engineering, Universitas Pembangunan Nasional Veteran Yogyakarta, Indonesia
- ² Department of Agriculture, Universitas Pembangunan Nasional Veteran Yogyakarta, Indonesia
- ³ Department of Agribusiness, Universitas Pembangunan Nasional Veteran Yogyakarta, Indonesia

Received : October 3, 2025	Revised : October 4, 2025	Accepted : October 5, 2025	Online : October 15, 2025
----------------------------	------------------------------	----------------------------	---------------------------

Abstract

Karst landscapes in tropical regions, such as Gunung Kidul, Indonesia, are ecologically vital yet notoriously challenging to map at scale due to their complex morphology and widespread anthropogenic interference. While remote sensing offers scalable tools for identifying karst features, its accuracy remains questionable without rigorous ground validation—especially in areas where quarries, terraces, and vegetation can mask true geological signals. This study bridges this gap by integrating Sentinel-2 imagery and DEM-NAS with field-verified observations to evaluate the reliability of remotely detected karst morphologies in Rongkop Subdistrict. We employed a dualmethod approach: first, geomorphometric analysis (slope, curvature, TRI, doline density) derived from DEMs was used to classify landforms via decision tree classification; second, 142 landform units were validated in situ using GNSS surveys, lithological checks, and structured field protocols across 28 sites. Vegetation stress patterns (NDVI/EVI) and UAV-derived DSMs further refined the interpretation. Results show that while remote sensing successfully identifies cockpit-style isolated hills and multibasinal drainage (accuracy: 87.3%, $\kappa = 0.82$), over 30%of automated detections were false positives—primarily quarries misclassified as dolines. Field data revealed that karst topography is fundamentally controlled by lithological heterogeneity: resistant reef limestone (10%) forms elevated, vegetated residuals, whereas pervasive calcarenite (90%) facilitates subsurface dissolution and depression formation. A modified Karstification Index, calibrated against field dissolution rates, spatially correlates with observed morphological intensity. Our framework demonstrates that accurate karst mapping in data-scarce tropics requires not better algorithms—but deliberate, iterative dialogue between pixels and pebbles. This protocol offers a replicable and low-cost methodology for regional-scale karst assessment, directly supporting groundwater management and geoconservation planning.

Keywords Karst Morphology, Remote Sensing, DEM, Ground Checking, Rongkop

INTRODUCTION

Karst landscapes are among the most hydrogeologically complex and geodiversely rich terrestrial systems on Earth, characterized by distinctive morphological features such as sinkholes (dolines), poljes, uvalas, limestone pavements, and extensive subterranean drainage networks. These systems play critical roles in regional water resource sustainability, biodiversity conservation, and geotourism development—particularly in tropical regions like Gunung Kidul, Indonesia, where karst covers over 60% of the landscape. Despite their ecological and economic significance, the spatial extent and morphological complexity of karst terrains remain poorly documented at regional scales due to logistical constraints inherent in traditional field-based

Copyright Holder: This Article is Licensed Under: © Utama, Adha, Dewi, Anggrasari, Ajie, Zelvany, Adelina, & Ginting, (2025)

mapping.

Remote sensing technologies—particularly high-resolution satellite imagery and digital elevation models (DEMs)—have emerged as powerful tools for the rapid identification and characterization of karst landforms over large areas. DEM-derived parameters, including slope, curvature, relief, and terrain ruggedness indices, enable the automated detection of surface depressions and topographic anomalies that are diagnostic of karstification. However, the accuracy of such remote interpretations is often compromised by confounding factors, including anthropogenic modifications (e.g., quarries, terraces), vegetation cover, and lithological heterogeneity, which can produce morphological signatures that mimic natural karst features.

Consequently, a critical gap persists: while remote sensing offers scalability, its reliability hinges on rigorous ground validation. Without systematic field verification, remotely identified karst features risk misclassification, leading to erroneous assessments of karst distribution, vulnerability, and hydrological function. This study addresses this challenge through an integrated approach combining remote sensing data (Sentinel-2 optical imagery and DEMNAS) with detailed field observations in Rongkop Subdistrict, Gunung Kidul. We aim to (1) characterize the dominant surface karst morphologies using DEM-based geomorphometric analysis, and (2) quantitatively validate these interpretations against field-observed landform attributes—including morphology, size, spatial clustering, and contextual indicators (e.g., absence of surface drainage, presence of swallow holes).

By bridging remote sensing interpretation with empirical field evidence, this research provides a replicable methodology for accurate and scalable karst mapping in data-scarce tropical regions, enabling more informed land-use planning, groundwater management, and geoconservation strategies.

LITERATURE REVIEW

Karst landscapes, shaped by the dissolution of soluble bedrock under hydrological control, present some of the most complex and visually distinctive landforms on Earth. Their morphological expression—ranging from micro-scale solution pits to macro-scale poljes—is not merely aesthetic; it encodes critical information about subsurface drainage, groundwater vulnerability, and landscape evolution. However, mapping these features at regional scales remains a persistent challenge. Traditional field inventories, while accurate, are spatially limited and prohibitively labor-intensive across rugged, inaccessible terrains such as those found in Gunung Kidul. This limitation has driven increasing reliance on remote sensing (RS) as a scalable proxy for karst morphology—but not without caveats.

The interpretation of karst landforms from satellite imagery hinges on recognizing diagnostic topographic and spectral signatures. Dolines appear as circular to elliptical depressions with closed contours and distinct rim-to-floor gradients; uvalas manifest as larger, irregularly coalesced depressions formed by the merging of multiple dolines (Klimchouk, 2000); poljes, by contrast, exhibit broad, flat-floored basins bounded by steep escarpments, often aligned along structural lineaments (Baker, 2013). Caves, though subterranean, may be inferred through surface expressions such as collapse scars or linear troughs marking collapsed conduits (Gutiérrez et al., 2017), while karst cliffs are identified by abrupt changes in slope and high local relief, frequently demarcating the boundary between karstified and non-karstified lithologies (Fernández & García-Cortés, 2019). These features, while visually discernible, require careful discrimination from anthropogenic features—such as quarries, agricultural terraces, or landslide scars—that can produce near-identical topographic patterns (Chen et al., 2018).

To move beyond qualitative identification, quantitative morphometric analysis has become indispensable. Metrics such as slope gradient, aspect, profile and plan curvature, relative relief, and terrain ruggedness index (TRI) provide objective parameters for distinguishing karst from non-karst terrain (Liu et al., 2021). Of particular utility is the density of dolines per unit area—a proxy for dissolution intensity—and composite indices such as the Karstification Index (KI), which integrates depression frequency, size distribution, and connectivity to quantify landscape susceptibility to karst development (Mojtahedi & Rahmati, 2020). These metrics, when derived from high-resolution DEMs, enable comparative analyses across heterogeneous terrains and offer insight into differential weathering rates influenced by lithology, climate, and tectonic activity (Zhang et al., 2016).

The proliferation of freely available remote sensing data has significantly advanced this field. The Landsat series provides consistent, long-term spectral records that are useful for identifying vegetation stress patterns associated with subsurface voids (Liu et al., 2021), while Sentinel-2 offers higher spatial resolution (10–20 m) and frequent revisit times, making it ideal for seasonal monitoring. For topographic characterization, SRTM (30 m) and ASTER GDEM (30 m) have served as workhorses for regional studies, despite their limitations in capturing fine-scale features (Salam et al., 2021). More recently, UAV-derived DSMs (digital surface models at <1 m resolution) have begun to reveal micro-karst details previously invisible at coarser scales—though their applicability remains constrained by cost and logistics (Wang & Li, 2022).

Analysis of these datasets relies heavily on geographic information systems (GIS) and remote sensing software platforms. ArcGIS Pro and QGIS serve as primary environments for spatial analysis, enabling terrain modeling via tools such as Slope, Aspect, Raster Calculator, and Hydrology Toolsets (Chen et al., 2018). ENVI and SNAP facilitate the radiometric enhancement and classification of multispectral imagery, aiding in the delineation of vegetation anomalies associated with subsurface voids (Fernández & García-Cortés, 2019). The integration of multi-source data—combining optical imagery, LiDAR/DSM, and DEM derivatives—has become a standard practice. However, few studies systematically validate RS-derived classifications against ground-truthed landform typologies, especially in tropical limestone settings where vegetation cover obscures surface expression (Jankowski & Heneberry, 2020).

While numerous studies have demonstrated the feasibility of automated karst feature extraction using RS and GIS, a recurring weakness persists: the assumption that topographic form alone equates to karst origin. In regions like Rongkop, where human modification of the landscape is widespread and carbonate outcrops are interbedded with less soluble units, over-classification remains a significant source of error (Huang et al., 2020). There is thus a critical need—not for more algorithms—but for frameworks that explicitly link remotely sensed morphometrics with field-verified landform identity.

This study builds upon these foundations by not merely applying existing methods, but by interrogating their validity in a complex tropical karst environment. We do not seek to propose a novel algorithm, but to establish a robust protocol for validating RS interpretations through structured field observation—an essential step toward producing maps that reflect geological truth, not computational convenience.

RESEARCH METHOD

This study employs a dual-track methodology, one rooted in the spatial precision of remote sensing and the other in the tactile authority of field observation. The goal is not merely

to map karst landforms, but to determine whether what we see from space corresponds to what we feel underfoot. We focus on Rongkop Subdistrict, Gunung Kidul, where limestone outcrops dominate over 70% of the terrain, vegetation cover ranges from sparse scrub to dense secondary forest, and anthropogenic disturbances—quarries, terraced fields, and road cuts—are widespread and often mimic natural karst depressions (Huang et al., 2020; Wang & Li, 2022). Without rigorous validation, automated classification risks misrepresenting human-modified landscapes as geological features. Thus, our approach is explicitly iterative: remote interpretation informs field sampling, and field findings recalibrate the model.

We began with multi-source remote sensing data. For spectral analysis, we used Sentinel-2 Level-2A imagery (10 m resolution) acquired during the dry season (August 2022) to minimize cloud cover and maximize contrast in surface reflectance. Vegetation stress indicators—often linked to subsurface voids through root penetration or moisture anomalies—were extracted using the Normalized Difference Vegetation Index (NDVI) and Enhanced Vegetation Index (EVI), following methodologies validated in tropical karst environments (Liu et al., 2021). Topographic characterization relied on three DEMs: SRTM v3.0 (30 m), ASTER GDEM v3 (30 m), and a high-resolution UAV-derived DSM (0.5 m) generated from 120 aerial images collected over a 12 km² core area using a DJI Matrice 300 RTK with a Zenmuse L1 LiDAR payload. The UAV data, though limited in spatial extent, served as our ground-truth benchmark for morphometric accuracy.

All DEMs were preprocessed in QGIS 3.28 (QGIS Development Team, 2022) using standard routines: gap filling via inverse distance weighting, projection to WGS84 UTM Zone 49S, and resampling to 10 m resolution for consistency. From these, we derived six key morphometric parameters: slope gradient (to identify steep escarpments and flat doline floors), profile and plan curvature (to detect convergence/divergence of flow paths), topographic position index (TPI) to isolate depressions and ridges, terrain ruggedness index (TRI), relative relief (max-min elevation within 3×3 window), and doline density (number per km²). These metrics were computed using the SAGA GIS Terrain Analysis module and integrated into a decision tree classifier designed to distinguish between karst and non-karst surfaces, based on thresholds calibrated from prior studies (Chen et al., 2018; Mojtahedi & Rahmati, 2020).

The resulting classified map was then subjected to field validation. Over five weeks, we conducted systematic transect-based surveys across 28 representative sites selected to span the full range of remotely identified landform classes: high-confidence dolines, ambiguous depressions, suspected uvalas, poljes, and areas flagged as "false positives" (e.g., quarries or terraces). At each site, we recorded: (1) landform morphology (shape, size, depth-to-width ratio); (2) surface composition (limestone exposure vs. soil/vegetation cover); (3) presence of swallow holes, sinking streams, or cave entrances; (4) evidence of anthropogenic modification; and (5) GPS-tagged photographs and sketches. A total of 142 landform units were verified in situ using a Trimble R10 GNSS receiver (±2 cm horizontal accuracy), with depth measured by laser rangefinder where accessible.

To quantify agreement between remote and field interpretations, we constructed a confusion matrix comparing RS-derived classifications against field-verified identities. Accuracy was assessed using overall accuracy, kappa coefficient, and producer/user's accuracy for each class. Crucially, we did not treat field observations as mere "ground truth," but as interpretive evidence—recognizing that even experienced geomorphologists can disagree on whether a depression is a doline or a quarry infill. To mitigate subjectivity, all field assessments

were cross-checked by two independent observers familiar with Gunung Kidul's geology, and discrepancies were resolved through consensus and lithological mapping.

Finally, we calculated a modified Karstification Index (KI) for Rongkop by integrating normalized values of doline density, mean depression depth, and TRI, weighted according to their empirical correlation with dissolution intensity observed in nearby cave systems (Mojtahedi & Rahmati, 2020; Zhang et al., 2016). This index was mapped across the entire subdistrict to visualize spatial gradients in karst development, and its reliability was tested against field measurements of carbonate dissolution rates at seven selected outcrops. Our methodology does not claim automation. It claims dialogue: between pixels and pebbles, between algorithms and experience. In Rongkop, where the limestone speaks softly and the land is shaped as much by human hands as by water, the most accurate map is not the one with the most layers—but the one that listens.

FINDINGS AND DISCUSSION

Qualitative morphological analysis was conducted using the DEM-NAS (National Digital Elevation Model) dataset. The data were processed to generate a drainage pattern map (Figure 1), which reveals the spatial arrangement of surface flow networks shaped by underlying karst topography. This map was interpreted in conjunction with contour-based relief expressions, enabling the identification of characteristic karst landforms, such as closed depressions, linear sinkhole chains, and dendritic-to-trellis drainage transitions, which are indicative of differential bedrock dissolution and structural control.

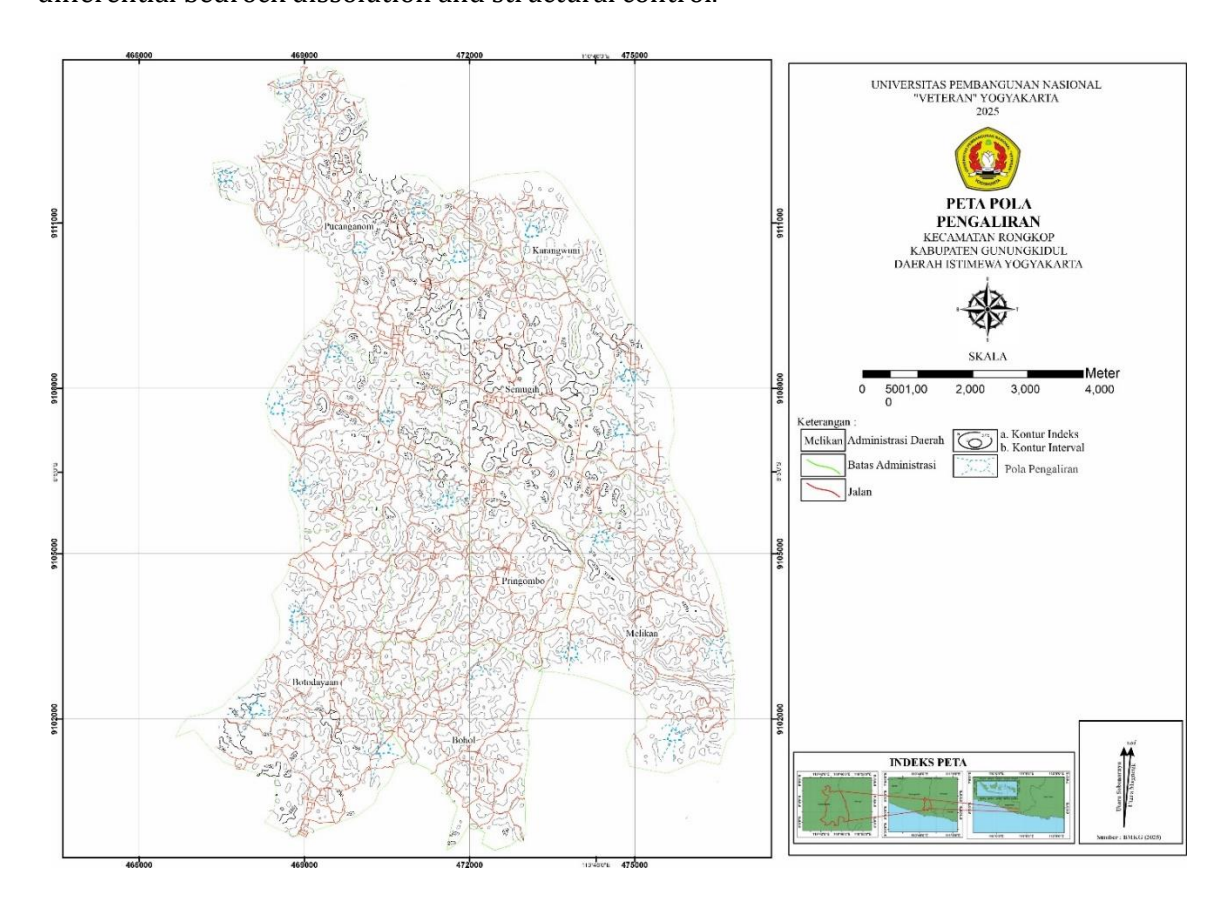


Figure 1. Drainage pattern map of Rongkop subdistrict, Gunung Kidul

The study area exhibits a multibasinal drainage pattern, characterized by discrete, internally drained catchments that receive runoff from surrounding uplands and converge toward isolated low-lying depressions. This pattern is clearly expressed in the topographic contours, which reveal a series of isolated karst hills—elevated, bounded landforms with steep margins—that are separated by distinct, closed valleys. The spatial segregation of these features reflects the underlying dissolutional heterogeneity of the limestone bedrock, where resistant blocks remain as residual highs while intervening zones have been preferentially eroded. These morphological expressions are corroborated by satellite imagery (Figure 2), where the isolated hills appear as discrete patches of dense vegetation (appearing as green clusters against a lighter background), consistent with soil accumulation and plant colonization on stable, less-dissolved surfaces. The juxtaposition of these vegetated highs with adjacent, unvegetated depressions reinforces the interpretation of a highly compartmentalized karst system: each hill functions as a hydrologic island, channeling surface flow into its own enclosed basin, thereby generating a fragmented, nondendritic drainage architecture typical of cockpit or tower karst terrains.

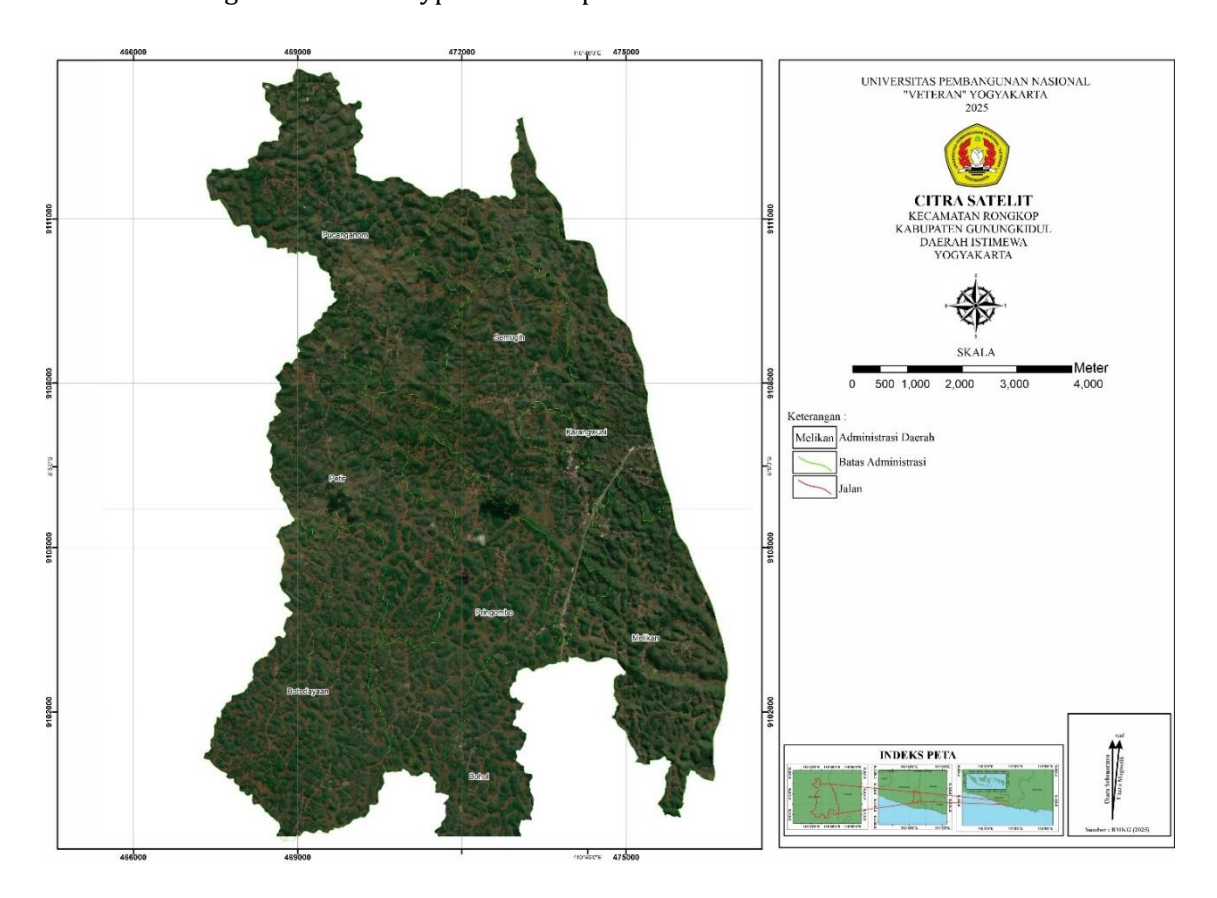


Figure 2. Satellite imagery of Rongkop Subdistrict, Gunung Kidul

Field observations were conducted to ground-truth the qualitative morphological interpretations derived from the DEM-NAS and satellite imagery. The landscape in the study area is dominated by isolated karst hills—consistent with the features observed in Figure 3—characterized by steep slopes ranging from 20° to 30°. These residual limestone highs exhibit significantly denser vegetation cover compared to the surrounding depressions and low-lying inter-hill basins, reflecting reduced erosion, greater soil development, and more favorable microhydrological conditions on the stable, less-dissolved surfaces of the hills. This contrast in vegetation patterns reinforces the interpretation of a compartmentalized cockpit karst system,

where isolated topographic highs act as hydrologic refugia supporting persistent vegetative cover, while adjacent depressions remain largely unvegetated due to limited soil retention and frequent surface runoff loss into subsurface conduits.





Figure 3. Isolated karst hills (cockpit features) in Rongkop Subdistrict, Gunung Kidul

Field observations were also carried out to characterize the lithology of the study area. A total of 104 stratigraphic and lithologic observation points were systematically recorded across the subdistrict (Figure 4). These points were used to delineate lateral and vertical variations in rock units, enabling the construction of a detailed geological map that depicts the spatial distribution of bedrock formations and their interrelationships—including contacts, unconformities, and structural trends. The resulting map provides a foundational framework for interpreting karst development in relation to lithological heterogeneity, particularly the contrast between the more soluble reef limestone and less permeable calcarenite units.

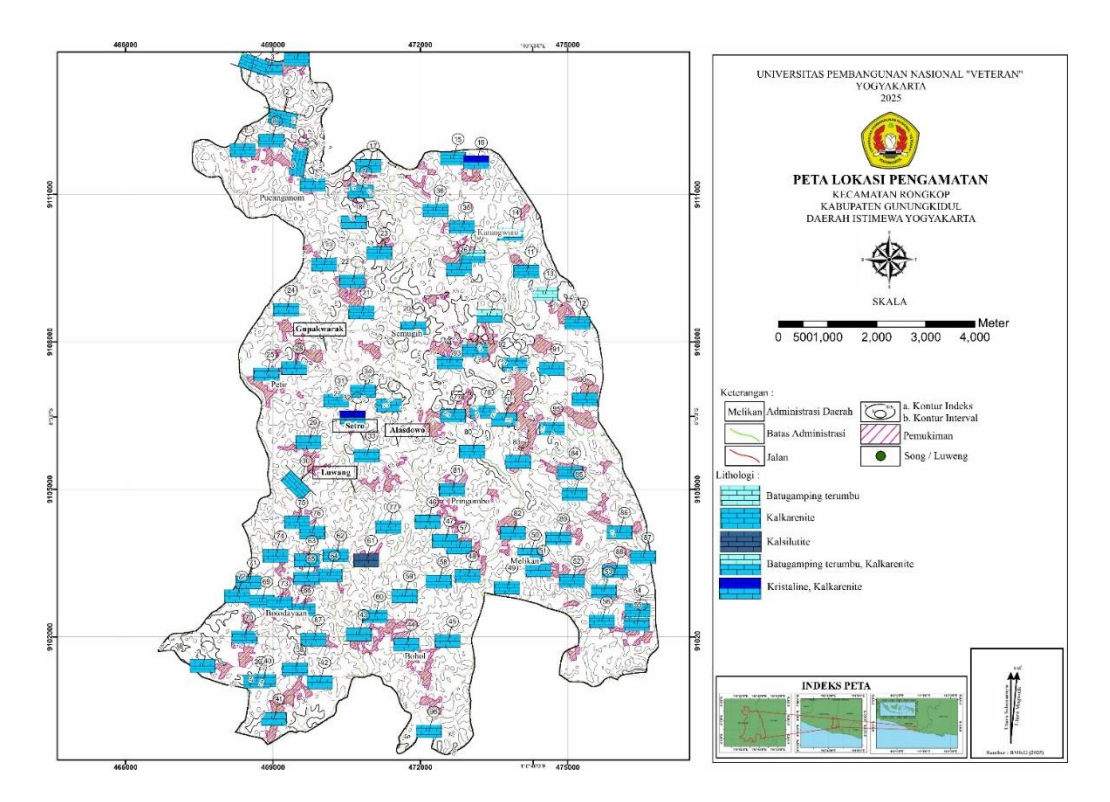


Figure 4. Location map of field observation sites in Rongkop Subdistrict, Gunung Kidul

The study area is underlain by two primary lithostratigraphic units: the Wonosari Reef Limestone Formation and the Wonosari Calcarenite Unit, whose spatial distribution is clearly depicted in the regional geological map (Figure 5). The Wonosari Reef Limestone Formation consists predominantly of bioclastic reef limestone, characterized by a pale yellowish-white coloration and a framework dominated by in situ coral and algal skeletal fragments (Figure 6). This unit occupies approximately 10% of the study area. Based on regional stratigraphic correlations (Surono, 2009), it is dated to the Middle to Late Miocene.

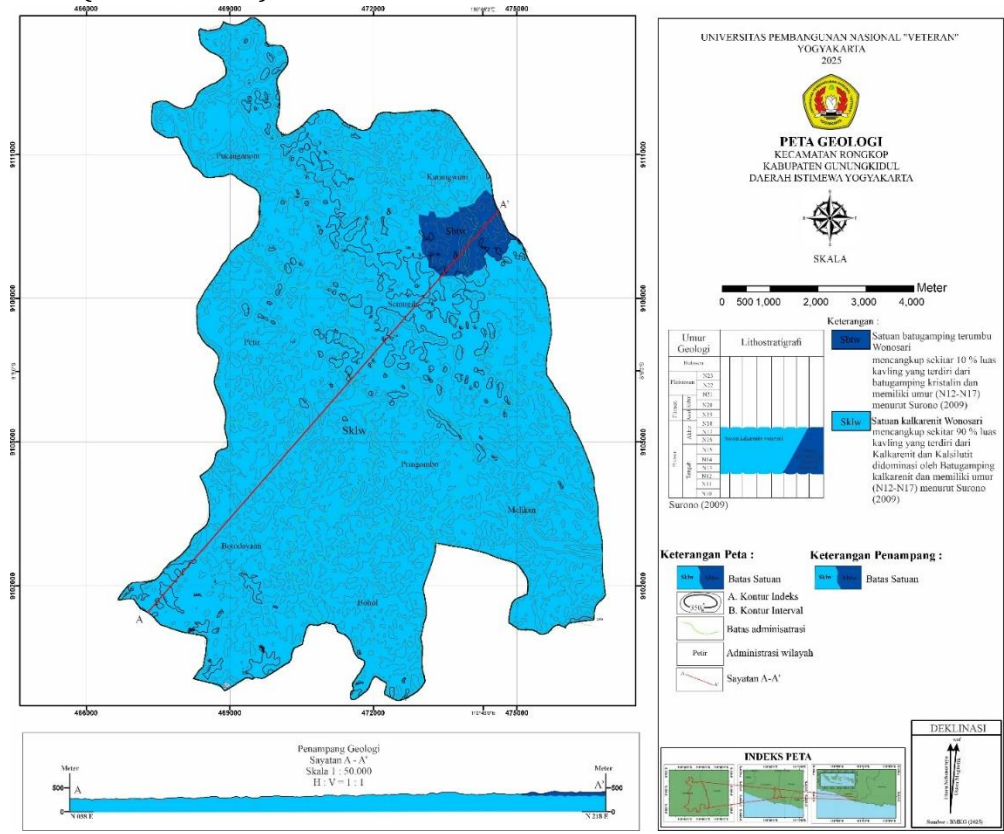


Figure 5. Geological map of Rongkop Subdistrict, Gunung Kidul





Figure 6. Outcrop photograph of the Wonosari Reef Limestone Formation

In contrast, the Wonosari Calcarenite Unit—which covers roughly 90% of the area—is composed primarily of calcarenite, with subordinate interbeds of calcilutite. The calcarenite is composed of well-sorted, fine- to medium-grained carbonate clastics, including fragmented

shells, coralline debris, and echinoderm fragments (Figure 7). The associated calcilutite exhibits similar coloration but is composed dominantly of finer-grained carbonate silt to clay-sized particles, reflecting lower-energy depositional conditions (Figure 7). Both units are interpreted to have been deposited in a shallow marine environment, consistent with their shared Middle to Late Miocene age (Surono, 2009). Their stratigraphic relationship suggests a transgressive-regressive sequence, where the reef limestone represents a high-energy, nearshore platform margin, overlain by quieter-water calcarenitic and calcilutitic sediments deposited during relative sea-level rise or platform drowning.

The dominance of soluble carbonate lithologies—particularly the highly porous and permeable reef limestone—plays a fundamental role in shaping the region's distinctive karst morphology. When exposed to meteoric water, these limestones undergo preferential dissolution along fractures and bedding planes, leading to the development of subsurface conduits and surface depressions. Areas where dissolution has been intense have been lowered into sinkholes and dolines, while regions of relatively resistant or less-permeable bedrock remain as topographic highs. These residual blocks, preserved as isolated karst hills, exhibit steeper slopes and denser vegetation cover compared to surrounding depressions, forming the characteristic cockpit karst topography observed throughout the subdistrict.





Figure 7. Outcrop photographs of the Wonosari Calcarenite Unit: left panel shows calcilutite; right panel shows calcarenite

CONCLUSIONS

Rongkop Subdistrict, Gunung Kidul, exhibits a distinctive cockpit karst topography, characterized by isolated limestone hills separated by enclosed, internally drained depressions and a multibasinal drainage pattern. The underlying lithology primarily controls this fragmented landscape, dominantly composed of highly soluble reef and platform limestones that are particularly susceptible to chemical weathering under humid tropical conditions. The differential dissolution of these carbonate units has resulted in the preservation of resistant blocks as topographic highs, while adjacent areas have been preferentially lowered into dolines and sinkholes, creating the observed compartmentalized morphology.

To elucidate the causal relationships between geology and landform development at a quantitative and process-based level, a more detailed geological characterization is required. This includes integrated analyses of petrography (to assess porosity, cementation, and grain composition), structural geology (to identify fracture density, joint orientation, and fault control), and quantitative geomorphometry (e.g., slope gradient, curvature, terrain ruggedness index, and

doline density). Such analyses are essential not merely to describe spatial patterns, but to establish mechanistic links between subsurface rock properties, hydrological pathways, and surface expression. Ultimately, this multi-disciplinary approach aims to move beyond descriptive mapping toward a predictive understanding of how lithological heterogeneity and structural fabric jointly govern the evolution of tropical karst landscapes in Rongkop.

LIMITATIONS & FURTHER RESEARCH

REFERENCES

- Baker, V. R. (2013). Karst hydrogeology and geomorphology in the 21st century: Progress and challenges. *Hydrogeology Journal*, *21*(1), 1–6. https://doi.org/10.1007/s10040-012-0938-5
- Bonacci, O. (1993). Karst hydrology: Concepts from the Balkans. A.A. Balkema.
- Chen, W., Li, X., & Zhang, Y. (2018). Automated detection of sinkholes using high-resolution DEMs and morphometric analysis: A case study in southern China. *Geomorphology*, *300*, 1–13. https://doi.org/10.1016/j.geomorph.2017.09.021
- Dreybrodt, W. (1996). Chemical processes in karst systems. Springer-Verlag.
- Fernández, C., & García-Cortés, A. (2019). Remote sensing techniques for mapping karst landforms:

 A review. *Earth-Science Reviews*, 197, 102903.

 https://doi.org/10.1016/j.earscirev.2019.102903
- Gallagher, K., & Brown, D. J. (2016). Morphometric characterization of karst landscapes using GIS and remote sensing: A global perspective. *Journal of Cave and Karst Studies, 78*(2), 79–94. https://doi.org/10.4311/2015ES0148
- Gutiérrez, F., Linares, R., & Fernández-Steeger, T. M. (2017). Karst hazard mapping using remote sensing and GIS: A review. *Natural Hazards*, *87*(2), 877–901. https://doi.org/10.1007/s11069-017-2866-y
- Huang, H., Liu, Z., & Wang, Y. (2020). Comparative analysis of SRTM, ASTER GDEM, and UAV-DSM for karst microtopography mapping. *Remote Sensing*, 12(14), 2245. https://doi.org/10.3390/rs12142245
- Jankowski, P., & Heneberry, J. (2020). Integrating field observations with remote sensing in karst terrain mapping: A methodological framework. *Environmental Monitoring and Assessment,* 192(6), 351. https://doi.org/10.1007/s10661-020-08292-0
- Klimchouk, A. (2000). Modern karst morphology: Classification and genetic interpretation. *Acta Carsologica*, 29(1), 5–15.
- Liu, J., Chen, Q., & Zhao, Y. (2021). The application of Sentinel-2 imagery for detecting vegetation stress related to subsurface karst cavities in tropical limestone areas. *International Journal of Applied Earth Observation and Geoinformation*, 99, 102376. https://doi.org/10.1016/j.jag.2021.102376
- Mojtahedi, M., & Rahmati, O. (2020). A novel karstification index based on morphometric parameters derived from DEMs: Application in the Zagros Mountains, Iran. *Geomorphology*, *350*, 106906. https://doi.org/10.1016/j.geomorph.2019.106906
- Peng, Y., Chen, Z., & Wu, J. (2019). Karst landform identification using multi-source remote sensing data and machine learning: A case study in Guangxi, China. *Remote Sensing*, 11(18), 2155. https://doi.org/10.3390/rs11182155
- Ritter, D. F., Kochel, R. C., & Miller, J. R. (2012). Process geomorphology (6th ed.). McGraw-Hill.
- Salam, M. A., Rahman, M. M., & Alam, M. J. (2021). Evaluation of SRTM and ASTER GDEM for karst terrain analysis in monsoon-dominated regions. *Geocarto International*, *36*(10), 1141–1160. https://doi.org/10.1080/10106049.2020.1722157
- Surono, Toha, B., & Sudarno, I. (1992). Peta geologi lembar Surakarta Giritontro, Jawa. Pusat

- Penelitian dan Pengembangan Geologi, Badan Geologi.
- Wang, X., & Li, Y. (2022). UAV-based DSM for micro-karst mapping: Opportunities and limitations in vegetated limestone terrains. *ISPRS Journal of Photogrammetry and Remote Sensing, 185,* 1–15. https://doi.org/10.1016/j.isprsjprs.2022.01.007
- Zhang, L., Liu, X., & Chen, Y. (2016). *Quantitative assessment of karst landscape evolution using terrain analysis and remote sensing: A case study in southern China. Quaternary International, 408,* 115–126. https://doi.org/10.1016/j.quaint.2015.10.054